Multimedia Tools and Applications (2023) 82:19993–20014
https://doi.org/10.1007/s11042-022-14259-z

An efficient compression technique for Foetal phonocardiogram signals in remote healthcare monitoring systems

Islam S. Fathi[1] · Mohamed Ali Ahmed[1] · M. A. Makhlouf[2,3]

Received: 31 May 2022 / Revised: 2 November 2022 / Accepted: 8 November 2022 /
Published online: 28 November 2022

Abstract
Remote Healthcare Monitoring Systems (RHMs) that employ fetal phonocardiography (fPCG) signals are highly efficient technologies for monitoring continuous and long-term fetal heart rate. Wearable devices used in RHMs still face a challenge that decreases their efficacy in terms of energy consumption because these devices have limited storage and are powered by batteries. This paper proposes an effective fPCG compression algorithm to reduce RHM energy consumption. In the proposed algorithm, the Discrete Orthogonal Charlier Moment (DOCMs) is used to extract features of the signal. The householder orthonormalization method (HOM) is used with the Charlier Moment to overcome the propagation of numerical errors that occur when computing high-order Charlier polynomials. The proposed algorithm's performance is evaluated in terms of CR, PRD, SNR, PSNR, and QS and provides the average values 18.33, 0.21, 48.85, 68.86, and 90.88, respectively. The results of the comparison demonstrate the proposed compression algorithm's superiority over other algorithms. It also tested in terms of compression speed and computational efficiency. The results indicate that the proposed algorithm has a high Compression speed (218.672 bps) and high computational efficiency (21.33). Additionally, the results reveal that the proposed algorithm decreases the energy consumption of a wearable device due to the transmission time decreasing for data by 3.68 s.

✉ Islam S. Fathi
i_said76@yahoo.com

Mohamed Ali Ahmed
Mohamed_ibrahim1@science.suez.edu.eg

M. A. Makhlouf
m.abdallah@ci.suez.edu.eg

[1] Department of Mathematics, faculty of Science, Suez Canal University, Ismailia, Egypt

[2] Department of information system, faculty of computers and informatics, Suez Canal University, Ismailia, Egypt

[3] Faculty of Computer Science, Nahda University, Beni-Suef, Egypt

Keywords Remote healthcare monitoring systems · fPCG signal compression · Fetal phonocardiography (fPCG) · Charlier moments · Householder method · Energy efficiency

1 Introduction

Congenital heart defects are reported to be the cause of 26.5% percent of pregnancy-related deaths [45]. It has also been shown that improving maternal health care can prevent more than 80% of maternal fatalities and fetal distress. Women during pregnancy are periodically required to monitor fluctuations in fetal heart rate (FHR) and Follow up with doctors regularly [53]. As a result, in the 1960s, Electronic Fetal Monitoring (EFM) is a strong diagnostic technique for foetal heart rate (FHR). Nodaway, continuous and long-term fetal heart rate surveillance seems to be an essential approach for improving diagnostic accuracy [4]. The methods that can be used to monitor a fetal include a cardiotocography (CTG) [35, 36], fetal electrocardiography (fECG) [43], fetal magnetocardiography (fMC) [50] or fetal phonocardiography (fPCG) [39, 48]. The fPCG approach appears to be one of the most effective prenatal methods based on foetal acoustic heart sounds (fHSs). [44]. Fetal phonocardiography (fPCG) is a non-invasive way to detect fetal heart sounds by recording acoustic cardiac signals (fHSs). It records vibrational acoustic signals from the maternal abdomen surface [10, 16]. fPCG signal gives vital information on cardiac murmurs and the fetal heart rate (fHR), which is a crucial determinant of the fetus's health and well-being [7]. The fPCG is a very effective instrument for clinical practice because of its complete non-invasiveness. Besides that, there are many advantages to using fPCG approaches, including the examination is inexpensive; that no radiation is emitted to the mother or foetus.

Furthermore, the fPCG device is user-friendly, allowing even non-experts to record signals during the mother's long-term day or night recordings and then be analyzed to obtain a more overall understanding of the fetus's functionality [8]. Ultrasound and ultra-sonographic cardiotocography (CTG), two commonly used foetal monitoring techniques, may be detrimental to the foetus. The fECG can only be done in an existing emergency, despite the danger of infection. Consequently, fPCG is the most recommended and risk-free alternative approach for recording foetal heart activity [14]. For more accurate diagnostic information, it is necessary to record the fPCG signals for an extended period of time at a high sampling rate and resolution. It needs a lot of memory space, a long time to send information, and wide bandwidth. [23]. Clinical care systems and electronic monitoring using Remote Healthcare Monitoring Systems (RHMs) have been gaining importance in recent years [13]. In RHMs, A sensor is put on the belly of the mother to record fPCG signal and wirelessly send it to a smartphone application via Bluetooth. The application receives an fPCG signal and transmits it to a cloud server, demonstrating the various algorithms in order to detect and diagnose disease. Remote Monitoring Systems are a highly effective instrument for transmitting data remotely and making rapid diagnoses. Unfortunately, these systems continue to face problems that impair their efficiency. Energy consumption is considered one of the important problems faced by Remote Healthcare Monitoring Systems sensors. Since it runs on batteries, the device's memory and processing capabilities are limited. Extending battery life by reducing power energy usage is a necessary step in assuring continuous signal capture and monitoring [1, 30]. So, conserving these sensors' energy is a crucial problem facing RHMs. Traditionally, energy consumption in sensors is caused by data sensing, data processing, and data transmission. Data transmission is considered the primary reason for the wastage of energy, in which during data

sending and receiving, the wastage of power occurs [49]. The recorded signal data must be minimized using efficient compression techniques to reduce energy consumption. This motivated us to provide solutions to the problem of energy consumption in the devices of RHMs. For this reason, we addressed the fPCG signal data compression algorithm to decrease the size of the signal being stored or transmitted to overcome this problem.

In general, Various of algorithms are introduced for compressing biomedical signal [26] such as Electrocardiography (ECG) [37], Electromyography (EMG) [54], Electroencephalographic (EEG) [9, 47] and Salt sensitive Rat Blood Pressure signal [5]. Concerning PCG signals, several publications have appeared in recent years documenting. A. Bendifallah et al. present PCG signal compression methods based on dictionary and bitmask techniques. This method is applied to the bitstream produced by Set Partitioning [11]. Hong Tang et al. developed a novel PCG signals compression technique using sound repetition and vector quantization [51]. In a recent paper, Ying-Ren Chien et al. propose a deep convolutional autoencoder for PCG compression. In that technique, seven convolutional layers are used to compress the PCG signals into the feature maps at the encoder stage and at the decoder stage; the other seven convolutional layers are used to decompress the feature maps and obtain the reconstructed image signals [15]. Despite the author's knowledge, very few publications can be found in the literature dealing with the issue of fPCG signaling pressure, but it has gained prominence in recent years [44].

The Transform-based techniques widely used in medical applications such as image watermarking [40–42, 58] and signal compression [26]. Vibha Aggarwal et al. [6] introduced a compression technique for foetal phonocardiography (PCG) signal based on Discrete Cosine Transform (DCT) and Discrete Wavelet Transform (DWT). The results show that DWT performed better than DCT in high spatial resolution for Foetal PCG signals. In a recent paper by Samit Kumar Ghosh [29], a methodology based on transforms for compressing the foetal Phonocardiogram (fPCG) signal is proposed. Transform-based techniques such as Discrete Cosine Transform (DCT), Discrete Wavelet Transform (DWT), and Fast Walsh Hadamard Transform (FWHT) are used to decompose the fPCG signal. The results demonstrate the efficiency of the transform strategies in compressing fPCG signals. FWHT has a higher CR, whereas DWT produces good fidelity parameters with a comparable CR.

In recent years, one-dimensional and two-dimensional discrete orthogonal moments have been gaining importance because of their ability to represent signals and images well in various fields. The applications of discrete orthogonal moments include signal and image reconstruction [17, 19, 31], face recognition [46], image classification [2, 12], image watermarking [57], image encryption [56], images compression [24, 33, 55], signals compression [3, 21, 32]. Charlier moment (CMs) represents one type of discrete orthogonal moment [18, 38]. The experimental results obtained Charlier moments' efficacy as feature descriptors.

In our work, we propose a compression technique based on discrete Charlier moment for fPCG signals. In order to calculate out CMs, you have to compute kernel discrete orthogonal polynomials. Two major problems constrain the High-order computation of Charlier polynomials: The first problem is the fluctuation of polynomial values due to power, exponential and factorial functions. We use a recurrence relation completely independent of Charlier polynomials computation to solve this problem, which is no longer dependent on the factorial and power functions. The second problem is the propagation of numerical errors that occur when computing high-order Charlier polynomials (CPs), which destroys the orthogonality property of these polynomials. To overcome this problem, we propose using the Householder orthonormalization method (HOM) to maintain the orthogonality property of high-order

CPs. With the use of HOM, the computation of Charlier coefficients at higher orders becomes numerically more stable. This paper includes a number of important contributions, which can be stated as follows:

- Proposing an efficient fPCG signals compression technique to reduce energy consumption in Remote Healthcare Monitoring Systems.
- Presenting a stable compution version of Charlier Moments,which at high orders CPs avoid numerical error propagation and preserve the orthogonality property.

The rest of the paper consists of seven sections: In Section 2, DOCMs and CPs will be discussed. Section 3 is devoted to describing the proposed procedure for maintaining the orthogonality property of CPs. The proposed algorithm is introduced in Section 4. Section 5 illustrates the compression performance indicators. The experimental results of this work are summarized in Section 6, while the discussion is reported in Section 7. In Section 8, we present the conclusion of this paper.

2 Material and methods

2.1 Discrete orthogonal Charlier moment

The set of discrete orthogonal one-dimensional (1D) Charlier Moment (CMs) are defined as follows [59]:

$$CM_p = \sum_{x=0}^{N-1} C_p^{a_1}(x) S(x), p \leq N \tag{1}$$

where $s(x)$ indicates a 1D signal of size $1 \times N$, $C_p^{a_1}(x)$ are Charlier polynomials to order p and a_1 denotes the parameter of Charlier polynomial, which must be a strictly positive real number ($a_1 > 0$).

The reconstructed signal $S(x)$ is calculated from the inverse transformation of Charlier Moment as follows:

$$S(x) = \sum_{x=0}^{N-1} CM_P C_P^{a_1}(x), x = 0, 1, 2, \ldots, N-1 \tag{2}$$

Using the following matrix form decreases the time and complexity of 1D Charlier moment computations significantly:

$$CM_p = \mathrm{C}_p{}^T s = \begin{bmatrix} C_0(0) & C_0(1) & \ldots & C_0(N-1) \\ C_1(0) & C_1(1) & \ldots & C_1(N-1) \\ \vdots & \vdots & \vdots & \vdots \\ C_P(0) & C_P(1) & \ldots & C_p(N-1) \end{bmatrix} \times \begin{bmatrix} s(0) \\ s(1) \\ \vdots \\ s(\mathrm{N}-1) \end{bmatrix} \tag{3}$$

where C_p indicates Charlier polynomials of order p,s denotes $1 \times N$ signal vector.The following matrix relation determines the inverse transformation of CMs.

$$\mathrm{S} = CM_p \mathrm{C}_p \tag{4}$$

where CM_p and C_p are Charlier moments and Charlier Polynomials, respectively.

2.2 Computation of Charlier polynomials

The Charlier polynomials of order (p) are formulated using hypergeometric function as follows [18]:

$$C_p^{a_1} = {}_2F_0\left(-n, -x; -\frac{1}{a_1}\right) \tag{5}$$

where x, p = 0,1,2,...,∞, p is Charlier polynomial order, a_1 is the parameter of Charlier polynomial (a_1>0), and ${}_2F_0(.)$ is defined as:

$${}_2F_0(a, b; z) = \sum_{k=0}^{\infty} (a)_k (b)_k \frac{z^k}{k!} \tag{6}$$

The symbol $(a)_k$is defined:

$$(a)_k = a(a+1)(a+2)\ldots(a+k-1) = \frac{\Gamma(a+k)}{\Gamma(a)} \tag{7}$$

Where Γ(.) indicates the gamma function.

The Charlier polynomials satisfy an orthogonal relation of the form:

$$\sum_{x=0}^{N} C_n^{a_1}(x) C_m^{a_1}(y) \omega(x) = \rho(n)\delta_{nm} \tag{8}$$

Where $\omega(x)$ is the weight function of the DOCPs defined as:

$$\omega(x) = \frac{e^{-a1} a_1^x}{x!} \tag{9}$$

The squared norm of DOCPs is calculated as follows:

$$\rho(p) = \frac{p!}{a_1^p} \tag{10}$$

The orthonormalized CPs are defined by the square norm $\rho(p)$ and the weighted function $\omega(x)$ as follows:

$$C_p^{a_1}(x) = C_p^{a_1}(x) \sqrt{\frac{\omega(x)}{\rho(p)}} \tag{11}$$

Using Eqs. (6) and (11) computing the Charlier polynomials is time-consuming and leads to numerical instability. For this reason, researchers are developing recursive calculation methods to efficiently determine polynomials.

The discrete orthogonal Charlier polynomials CPs of order (p) are presented using recursive relation as follows [18].

$$C_p^{a_1}(x) = \frac{a_1 - x + p - 1}{a_1} \sqrt{\frac{\rho(p-1)}{\rho(p)}} C_{p-1}^{a_1}(x) - \frac{p-1}{a_1} \sqrt{\frac{\rho(p-2)}{\rho(p)}} C_{p-2}^{a_1}(x) \tag{12}$$

with $$c_0^{a_1}(x) = \sqrt{\frac{\omega(x)}{\rho(0)}} = \sqrt{\frac{e^{-a_1} a_1^x}{x!}}$$

$$C_1^{a_1}(x) = \frac{a_1 - x}{a_1}\sqrt{\frac{\omega(x)}{\rho(1)}} = \frac{a_1 - x}{a_1}\sqrt{\frac{e^{-a_1}a_1^{x+1}}{x!}} \tag{13}$$

The existence of the power, exponential and factorial functions that lead to the numerical fluctuations in the Charlier polynomials coefficients eliminates in the next section.

The following recurrence formula can be generated from the function $\rho(p)$ given by Eq. (10).

$$\begin{aligned} \rho(p+1) &= \frac{(p+1)}{a_1}\rho(p) \quad \text{with } \rho(0) = 1, \\ \frac{\rho(p-1)}{\rho(p)} &= \frac{a_1}{p} \text{ and } \frac{\rho(p-2)}{\rho(p)} = \frac{a_1^2}{p(p-1)}. \end{aligned} \tag{14}$$

Using Eqs. (14) and (12), we get:

$$C_p^{a_1}(x) = \frac{a_1 - x + p - 1}{a_1}\sqrt{\frac{a_1}{p}}C_{p-1}^{a_1}(x) - \sqrt{\frac{p-1}{p}}C_{p-2}^{a_1}(x) \tag{15}$$

with

$$\begin{aligned} C_0^{a_1}(x) &= \sqrt{\frac{e^{-a_1}a_1^x}{x!}} \\ C_1^{a_1}(x) &= \frac{a_1 - x}{a_1}\sqrt{\frac{e^{-a_1}a_1^{x+1}}{x!}} \end{aligned} \tag{16}$$

We observe that Eq. (15) presents a recurrence relation completely independent of the $\rho(p)$ function, indicating eliminating terms that numerically fluctuate the polynomial coefficients. The factorial, exponential, and power functions still exist in determining the initial conditions. To efficiently overcome these obstacles while computing $C_0^{a_1}(x)$ and $C_1^{a_1}(x)$ These initial conditions will be calculated as follows:

- for $p = 0$, we have from Eq. (16):

$$C_0^{a_1}(x+1) = \sqrt{\frac{e^{-a_1}a_1^x}{x!}}\sqrt{\frac{a_1}{x+1}} \tag{17}$$

Based on Eqs. (16) and (17), we get:

$$C_0^{a_1}(x+1) = \sqrt{\frac{a_1}{x+1}}C_0^{a_1}(x) \qquad \text{with} \qquad C_0^{a_1}(0) = e^{\frac{-a_1}{2}} \tag{18}$$

- for $p = 1$, we have from Eq. (16):

$$C_1^{a_1}(x+1) = \frac{a_1 - x + 1}{a_1}\sqrt{\frac{\omega(x+1)}{\rho(1)}} = \frac{a_1 - x + 1}{a_1}\sqrt{\frac{e^{-a_1}a_1^{x+2}}{(x+1)!}} \tag{19}$$

Based on Eqs. (16) and (19), we get:

$$C_1^{a_1}(x+1) = \frac{a_1 - x + 1}{a_1 - x}\sqrt{\frac{a_1}{x+1}}C_1^{a_1}(x) \text{ with } C_1^{a_1}(0) = \sqrt{e^{-a_1}a_1} \tag{20}$$

It is deterring the initial conditions using Eqs. (18) and (20) overcome the numerical fluctuations because of no longer dependent on the factorial and power functions. During the recursive calculation of CPs, numerical error propagation occurs due to the round-off error propagation. This error propagation leads to the loss of the orthogonality property of CPs. In order to find a solution to this problem, we propose in the next section to use the Householder orthonormalization method (HOM). The purpose of applying this procedure is to preserve the orthogonality property of CPs at high order during recursive calculations.

3 The proposed procedure for maintaining the orthogonality property of CPs using the householder method

According to the orthogonality property, CPs matrix ($C_{n,x}$) satisfies the following relation [20]:

$$C_{n,x}{}^T C_{n,x} = I_n \tag{21}$$

Where I_n is the identity matrix.

To avoid numerical error propagation and keep the property of orthogonality of CPs, we present a new method for re-orthonormalizing CPs matrix columns using QR decomposition methods. In these methods, a matrix $A = [u_1, u_2, \ldots, u_{n-1}, u_n]$ of size $n \times m$ factored as $A = QR$, where Q is an $n \times m$ matrix with orthogonal columns ($Q^TQ = I$) and R is an $m \times m$ upper triangular matrix [28]. In our situation, R matrix contains just recursive computation errors. The primary purpose of these methods is to generate the orthogonal $Q(n \times m)$ matrix from $C_{n,x}$ that contains round-off errors.

Many methods are used in QR decomposition, such as the Gram-Schmidt method, the Householder method, and the Given Rotations method. For QR decomposition of matrices, the Householder approach is considered numerically more stable and faster execution than the Gram-Schmidt and Given Rotations methods orthogonalization. As a result, the Householder approach is preferred for real-time applications [20]. The proposed algorithm for computing Charlier polynomials (CPs) using the Householder orthonormalization method (HOM) is illustrated in Algorithm 1:

Algorithm 1 The Proposed Algorithm for computing CPs using HOM

Inputs: N: the maximum value of the variable x; N_{max} : the order of CPs; a_1 : CPs parameter. **Output:** Q : the orthonormalized CPs matrix using HOM.	

Step 1	Compute $C_0^{a_1}(0)$ and $C_1^{a_1}(0)$ from Eqs. (18) and (20)
	for $x \leftarrow 0$ to $N-1$ **do**
	Compute $C_0^{a_1}(x+1)$ and $C_1^{a_1}(x+1)$ using Eqs. (18) and (20)
	end for

Step 2	**for** $x \leftarrow 0$ to $N-1$ **do**
	for $p \leftarrow 2$ to $N_{max}-1$ **do**
	Compute $C_p^{a_1}(x)$ using Eq. (15)
	end for
	$C = C_p^{a_1}(x)$

Step 3	**for** $i \leftarrow 1$ to N **do**
	$u = C_{i:N,i}$
	$v_i = sign(u_1)\|u\|_2 I_1 + u$
	$v_i = v_i / \|v_i\|_2$
	$Q_{i:N,i:N} = Q_{i:N,i:N} - 2v_i(v_i^T Q_{i:N,i:N})$
	end for
	end for

4 The proposed compression algorithm

The proposed algorithm is described as follows: the original fPCG signal (1 × N) is the input, and the fPCG signal is subdivided into smaller blocks of size (1 × n). In the proposed algorithm, we selected the size of blocks (1 × 125). The order (P) of the Charlier moment is selected according to the required compression factor (CF) as follows:

$$\text{Order(P)} = \text{Round}\left[\frac{\text{n}}{100-\text{CF}}\right], \tag{22}$$

Where compression factor (CF) shows how much of the signal is compressed. After determining the order (p), The Charlier polynomials (CPs) are computed on the signal block using Eq. (15). Then, the Householder method (HOM) is applied to the Charlier polynomials (CPs) as illustrated in algorithm 1. The forward Charlier moment is applied to the signal block to extract the discriminate features using Eq. (3). The features of the signal blocks are concatenated to obtain the compressed fPCG signal. In the decompression process, the compressed signal is subdivided into blocks, and the inverse transformation of CMs is applied to each block using Eq. (4). Then, the blocks are concatenated to obtain the reconstructed fPCG signal.

The main steps of the proposed compression algorithm are summarized as:

Step1: Input the fPCG signal to be compressed.
Step2: Input the desired CF, and Set block size (1 × n) = (1 × 125).
Step3: Determine the order (P) of the Charlier polynomials using Eq. (22).
Step4: Set the value of the parameter a_1 =140.
Step5: For each block.
Step6: Compute Charlier polynomials of order (p) by Eq. (15).

Step7: Apply the Householder method (HOM) on the Charlier polynomials (CPs) using algorithm 1.
Step8: Compute the forward Charlier moment by Eq. (3).
Step9: Concatenate the features of each block.
Step10: Apply the inverse transformation of the Charlier moment to obtain the reconstructed signal by Eq. (4).
Step11: Calculate the efficiency of the proposed algorithm by computing PRD, SNR, and PSNR.

Figure 1 show Digram that illustrates the processes of compression and decompression. Figure 2 show Flow chart for the proposed compression Fpcg signals algorithm. The proposed algorithm for compression fPCG signals can be summarized in Algorithm 2.

Algorithm 2 The proposed algorithm for compressing fPCG signals

Inputs: s: fPCG signal; block size (n) =125; desired CF; a_1 : CPs parameter value. Output: Compressed signal; Reconstructed signal; CR; PRD; SNR; PSNR; QS.
1. Subdivide the fPCG signal into smaller blocks of size (1×n). 2. Determine order (P) of Charlier Moment (CMs) (Eq. (22)). 3. For each block 4. Apply Algorithm 1 to compute Charlier polynomials (CPs). 5. Apply the Charlier Moment (CMs) to get the features (Eq. (3)). 6. End for 7. Concatenate the features of each block to get the compressed signal. 8. For each block 9. Apply the inverse of Charlier Moment (CMs) to the features to get a signal block (Eq. (4)). 10. Concatenate the signal blocks to get the reconstructed signal(S). 11. End for 12. Evaluate the proposed algorithm performance (CR, PRD, SNR, PSNR, QS).

5 Compression performance indicators

The effectiveness and efficiency of the presented compression algorithm are evaluated based on the following performance criteria. [22, 25]:

– Compression ratio (CR)

$$\mathrm{CR} = \frac{\text{number of bits for the original signal}}{\text{number of bits for the compressed signal}} \tag{23}$$

– Percent Root Mean Square Difference (PRD)

$$\mathrm{PRD} = \sqrt{\frac{\sum (s(x) - S(x))^2}{\sum s(x)^2}} \times 100 \tag{24}$$

where $s(x)$, $S(x)$ are the original and the reconstructed signal, respectively.

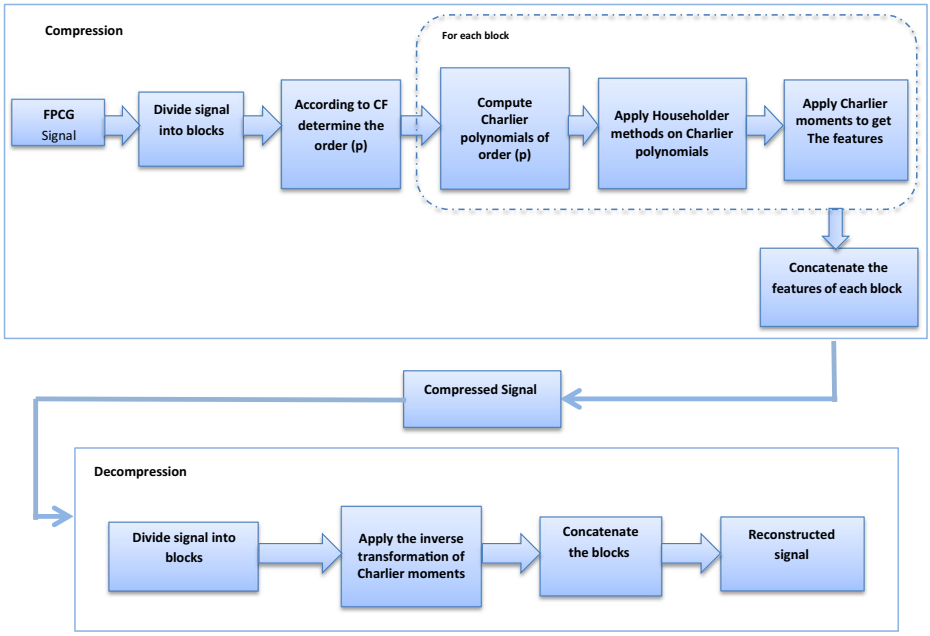

Fig. 1 Diagram of the proposed algorithm's compression and decompression steps

– Quality Score (QS)

QS is utilized to evaluate the overall performance of a compression technique. A high QS number indicates higher compression performance, as described below:

$$\mathrm{QS} = \frac{\mathrm{CR}}{\mathrm{PRD}} \tag{25}$$

– Signal to Noise Ratio (SNR)

$$\mathrm{SNR} = 10 \times \log\left(\frac{\sum\left(s(x)-\overline{s(x)}\right)^2}{\sum(s(x)-S(x))^2}\right) \tag{26}$$

where $\overline{s(x)}$ is the mean value of $s(x)$.

– Peak Signal to Noise Ratio (PSNR)

$$\mathrm{PSNR} = 20 \times \log_{10}\frac{max|s(x)|}{\sqrt{MSE}} \tag{27}$$

Where $max|s(x)|$ is the maximum point in $s(x)$, and MSE is the mean square error between the original $s(x)$ and reconstructed signal$S(x)$.

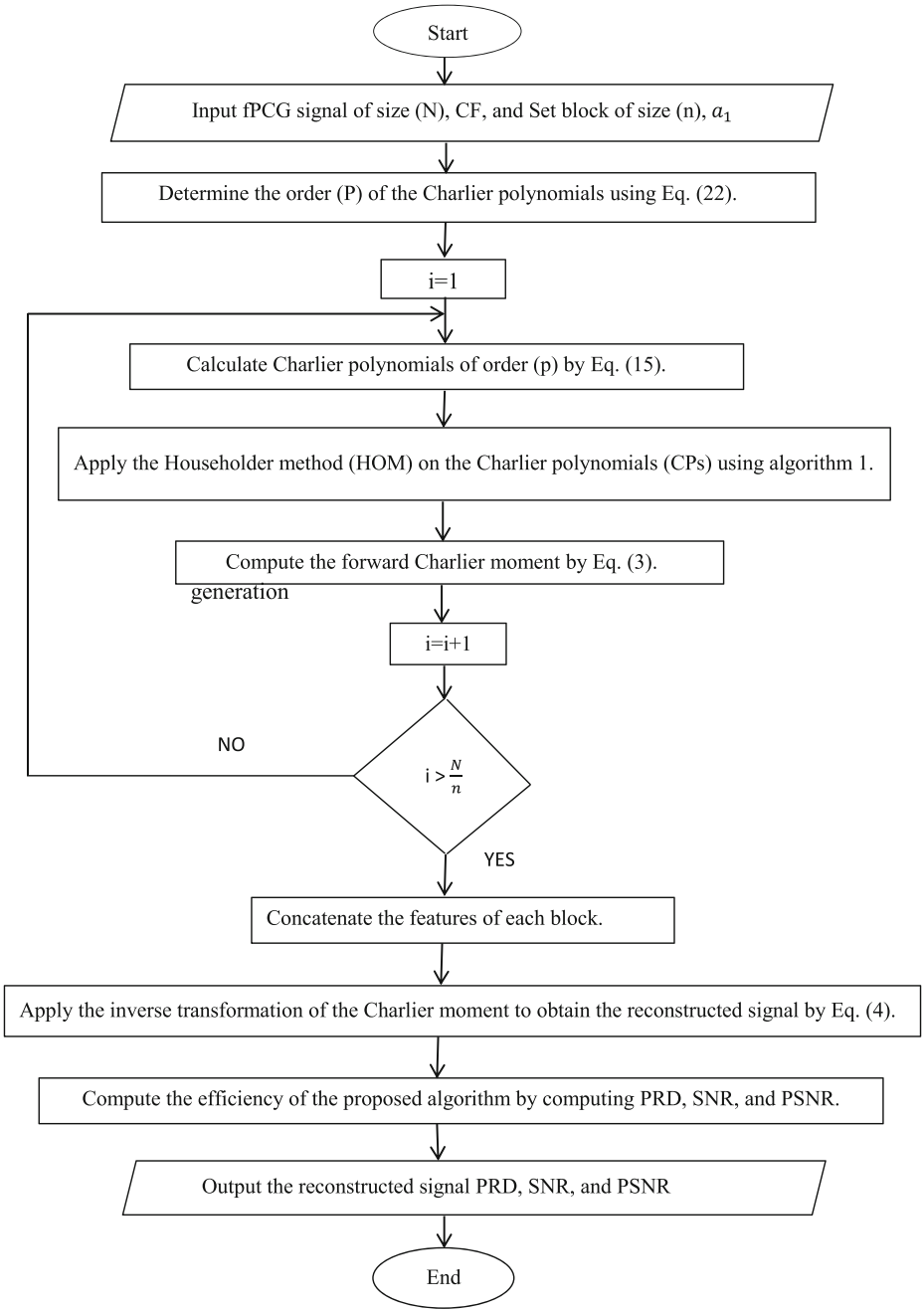

Fig. 2 Flow chart for the proposed compression Fpcg signals algorithm

– Compression Speed

$$\text{Compression Speed} = \frac{\text{uncompressed bits}}{\textit{sconds to comperss}} \tag{28}$$

$$\text{Decompression Speed} = \frac{\text{uncompressed bits}}{\textit{sconds to decomperss}} \tag{29}$$

– Computational efficiency (CE)

Computational efficiency (CE) is presented as CE of algorithm stands for the ratio between the Compression ratio and Processing Time. A high CE value indicates superior computational efficiency, which CE value reveals a high CR with a lower compression Time.

$$\text{CE} = \frac{\text{CR}}{\text{Compression Time}} \tag{30}$$

6 Experimental results

Fetal PCG Database was used to test the effectiveness of the proposed compression algorithm [34]. It contains 26 fPCG signals from pregnant women in their final months of physiological singleton pregnancies (weeks 31–40). The recorded samples were 1 minute (60 seconds) in duration, and the data were digitized at a sampling rate of 333 Hz at an 8-bit ADC. All of the ladies were healthy and between the ages of 25 and 35.

6.1 Results of the proposed algorithm

The performance compression of the proposed algorithm was evaluated using the Fetal PCG Database in terms of CR, PRD, SNR, PSNR, and QS. Table 1 summarizes the obtained results of the proposed algorithm on the Whole (26 signal) Fetal PCG dataset. From Table 1, observably, the proposed method yields excellent results for all signals in the dataset. It produces large compression ratios (CR), excellent reconstruction quality (PRD), and high SNR and PSNR. For particular fetal_PCG_p07_GW_38m signal, the proposed algorithm achieves large compression ratios (CR = 32) with large reconstruction quality (PRD = 0.17) and excellent PSNR (PSNR = 46.01). The fetal_PCG_p07_GW_38m, fetal_PCG_p11_GW_37m, and fetal_PCG_p23_GW_38m have the best Quality Score (QS) 188.24, 168.42, 145.45, respectively (A high QS result represents that the CR is high and the distortion rate is low). The proposed algorithm has an average performance of 18.33, 0.21, 48.85, 68.86, and 90.88 in terms of CR, PRD, SNR, PSNR, and QS, as depicted in Table 1. Figures 3, 4, 5 and 6 depict compressed and decompressed fPCG signals using the proposed method. Visual examination reveals that the reconstructed signals closely resemble the original signals.

Table 1 Compression performance indicators of the proposed algorithm for fPCG signals

FPCG signal	CR	PRD	SNR	PSNR	QS
fetal_PCG_p01_GW_36m	16	0.19	49.01	68.51	84.21
fetal_PCG_p02_GW_31m	8	0.13	49.92	75.38	61.53
fetal_PCG_p03_GW_37m	6.4	0.11	50.31	78.47	58.18
fetal_PCG_p04_GW_38m	32	0.28	48.10	61.63	114.28
fetal_PCG_p05_GW_34m	32	0.25	48.21	63.79	128
fetal_PCG_p06_GW_36m	21.4	0.19	49.01	68.49	112.31
fetal_PCG_p07_GW_38m	32	0.17	49.21	70.73	188.24
fetal_PCG_p08_GW_37m	16	0.31	47.88	59.91	51.62
fetal_PCG_p09_GW_40m	9.2	0.12	50.10	77.22	76.42
fetal_PCG_p10_GW_36m	21.3	0.21	48.90	67.63	101.42
fetal_PCG_p11_GW_37m	32	0.19	49.01	68.02	168.42
fetal_PCG_p12_GW_39m	16	0.19	49.01	68.51	84.21
fetal_PCG_p13_GW_36m	16	0.22	48.32	66.41	72.73
fetal_PCG_p14_GW_36m	10.6	0.52	45.53	51.42	20.5
fetal_PCG_p15_GW_36m	16	0.17	49.21	70.38	94.12
fetal_PCG_p16_GW_39m	21.3	0.24	48.25	64.92	88.75
fetal_PCG_p17_GW_35m	8	0.12	50.10	77.57	66.6
fetal_PCG_p18_GW_40m	8	0.16	49.41	71.33	50
fetal_PCG_p19_GW_38m	16	0.14	49.60	73.82	114.28
fetal_PCG_p20_GW_40m	16	0.23	48.30	65.02	69.56
fetal_PCG_p21_GW_39m	16	0.21	48.90	66.99	76.19
fetal_PCG_p22_GW_38m	10.6	0.14	49.60	73.42	75.72
fetal_PCG_p23_GW_38m	32	0.22	48.32	66.40	145.45
fetal_PCG_p24_GW_36m	21.3	0.33	47.86	59.20	64.54
fetal_PCG_p25_GW_37m	32	0.28	48.10	62.09	114.24
fetal_PCG_p26_GW_36m	10.6	0.13	49.92	75.11	81.54
Average	18.334	0.209	48.849	68.168	90.886

6.2 Results of comparisons between the proposed technique and existent compression algorithms

To the sake of validating the efficiency of the proposed approach, a comparative investigation is performed with existing compression algorithms [6, 29] in CR, PRD, and QS. The results obtained from the comparison of the proposed approach with transform-based techniques such as Discrete Cosine Transform (DCT), Discrete Wavelet Transform (DWT), and Fast Walsh Hadamard Transform (FWHT) are summarized in Table 2. As depicted in Table 2, for the

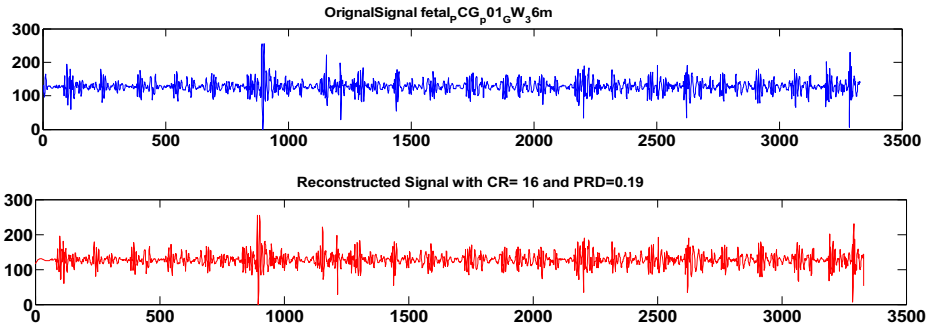

Fig. 3 Compression of fetal_PCG_p01_GW_36m signal with CR = 16 and PRD = 0.19

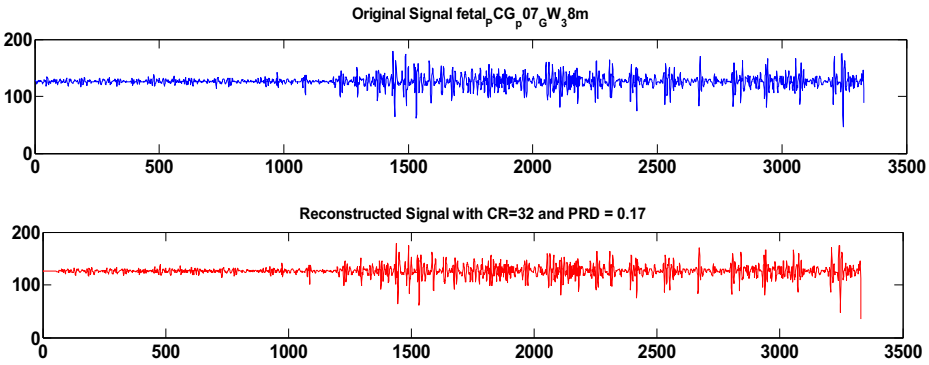

Fig. 4 Compression of fetal_PCG_p07_GW_38m with CR = 32 and PRD = 0.17

comparison with DCT and DWT, the proposed method outperforms them in all performance indicators for fPCG in the dataset. The proposed method has the highest QS because it has good CR and the lowest PRD. Comparing the proposed method to FWHT may not achieve the highest CR, but it achieves excellent PRD and the best QS.

Consequently, the proposed approach produces the greatest quality reconstructed signal compared to all other known techniques. This ensures that the reconstructed signal will contain all relevant diagnostic information. Figure 7 show a comparison of the proposed approach with DCT, DWT, and FWHT in term of SNR, PRD, CR, and QS, each of them independently. FWHT provides good results in CR, but the proposed algorithm is extremely high QS and better reconstruction quality (PRD). Graphs in Fig. 7 demonstrate the superiority of the proposed method compared to all other known techniques in SNR, PRD, and QS.

6.3 Compression speed and computational efficiency of the proposed algorithm

Table 3 summarises the Compression time, Compression speed, and computational efficiency for various fPCG signals extracted from datasets utilized in this paper and applied to the proposed approach. The proposed algorithm's compression time and compression speed are just as important as their compression performance. The compression speed of the technique is crucial for wireless biosensors in RHMs. As seen in Table 3, compression speed and computational efficiency increase as compression time decreases.

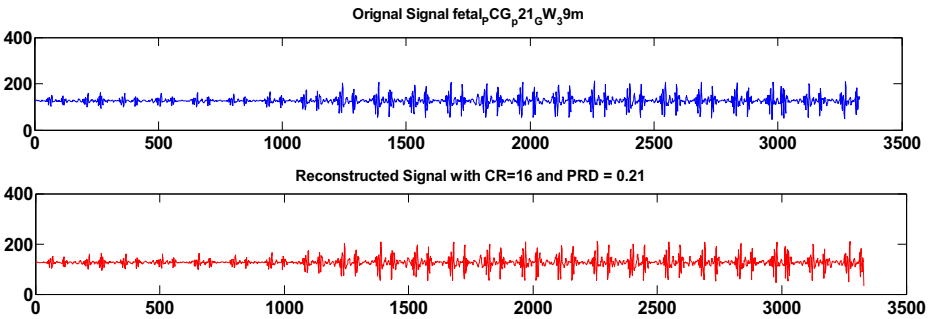

Fig. 5 Compression of fetal_PCG_p21_GW_39m with CR = 16 and PRD = 0.21

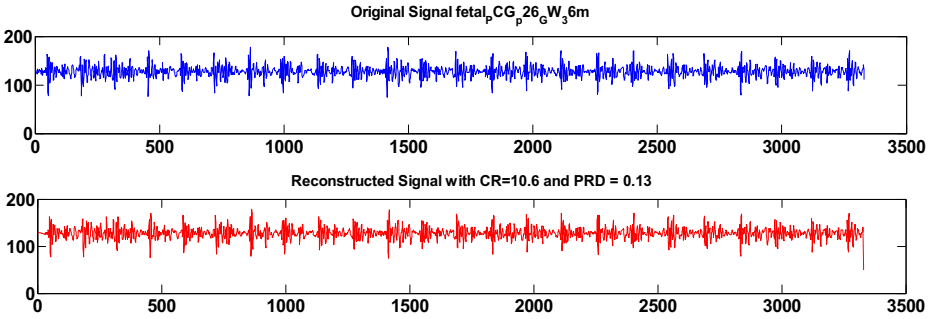

Fig. 6 Compression of fetal_PCG_p26_GW_36m with CR = 10.6 and PRD = 0.13

6.4 Energy consumption evaluation

This section discusses the evaluation energy consumption with the proposed algorithm. The proposed compression algorithm is implemented on STM32f429 Discovery development board. The STM32f429 discovery system comprises an ARM Cortex-M4base 32-bit microcontroller from STMicroelectronics. It operates at a maximum frequency of 180 MHz, which this study utilizes for data compression [27]. The development board offers a direct memory access technique (DMA) for fPCG measuring devices accessing memory directly. It is connected with a Bluetooth module with UART as compressed data output. Module-MD08R-C2A Bluetooth module with baudrate support of 1.2 k to 921.6 k bps is employed. The Bluetooth module is linked to the development board through the UART interface, and the baudrate is set to 230,400 bps (28,800 bytes).

- Wearable devices are in a "wake-up" state when processing or transmitting data; otherwise, they are in a "sleep" state.
- While a wearable device is in 'wake-up' mode, it drains battery power.
- Decreasing the transmitting data size reduces data transmission time, consequently reducing a 'wake-up' mode.
- Battery consumption is reduced by decreasing a 'wake-up' mode for the wearable device.
- According to the fPCG dataset mentioned above, the size of fetal_PCG_p01_GW_36m (333*8*60) = 159,840 bytes.
- Depending on the Bluetooth capability used, the transmission time of the signal is (159,840/28,880) 5.55 seconds.
- Table 3 indicates that the signal is compressed by CR = 16, and the compression time is 1.47 seconds, which means that the size of the compressed signal is 9990 bytes. Then the transmission time of the compressed signal is 0.347 seconds

Conditions	Compression Time(s)	Transmission Time(s)	total time(s)
without compression	–	5.55	5.55
with compression	1.47	0.347	1.817

From previous data, we note that the signal will be transmitted in *5.55* seconds; using the compression, the signal will be compressed and transmitted in 1.47 + 0.347 = 1.817. Therefore, the proposed compression algorithm decreases the overall work time by about 5.55–1.87 = 3.68 s.

Table 2 Compression performance comparison of the proposed algorithm with existing algorithms

FPCG signal	DCT			DWT			FWHT			Proposed algorithm		
	CR	PRD	QS	CR	PRD	QS	CR	PRD	QS	CR	PRD	QS
fetal_PCG_p01_GW_36m	5.42	0.51	10.62	5.58	0.53	10.53	27.49	0.5	54.46	16	0.19	84.21
fetal_PCG_p02_GW_31m	5.29	0.54	9.79	5.78	0.54	10.70	42.89	0.5	86.31	8	0.13	61.53
fetal_PCG_p03_GW_37m	5.27	0.52	10.13	5.40	0.52	10.38	–	–	–	6.4	0.11	58.18
fetal_PCG_p04_GW_38m	5.42	0.51	10.62	5.59	0.53	10.54	42.00	0.5	81.56	32	0.28	114.28
fetal_PCG_p05_GW_34m	5.92	0.51	11.61	5.58	0.53	10.52	43.86	0.5	87.77	32	0.25	128
fetal_PCG_p07_GW_38m	–	–	–	–	–	–	43.12	0.5	87.06	32	0.17	188.24
fetal_PCG_p09_GW_40m	5.33	0.52	10.25	5.49	0.53	10.36	–	–	–	9.14	0.12	76.16
fetal_PCG_p10_GW_36m	5.69	0.51	11.16	5.89	0.52	11.33	37.12	0.5	74.82	21.3	0.21	101.42
fetal_PCG_p11_GW_37m	–	–	–	–	–	–	39.10	0.5	77.44	32	0.19	168.42
fetal_PCG_p12_GW_39m	5.36	0.51	10.51	5.65	0.56	10.08	32.95	0.5	66.90	16	0.19	84.21
fetal_PCG_p17_GW_35m	5.68	0.52	10.93	5.87	0.52	11.28	–	–	–	8	0.12	66.6
fetal_PCG_p18_GW_40m	5.00	0.52	9.62	5.60	0.53	10.56	–	–	–	8	0.16	50
fetal_PCG_p21_GW_39m	–	–	–	–	–	–	29.19	0.5	58.29	16	0.21	76.19
fetal_PCG_p25_GW_37m	–	–	–	–	–	–	40.11	0.5	81.14	32	0.28	114.24
Average	5.44	0.51	10.52	5.67	0.53	10.63	37.77	0.5	75.75	19.21	0.18	97.99

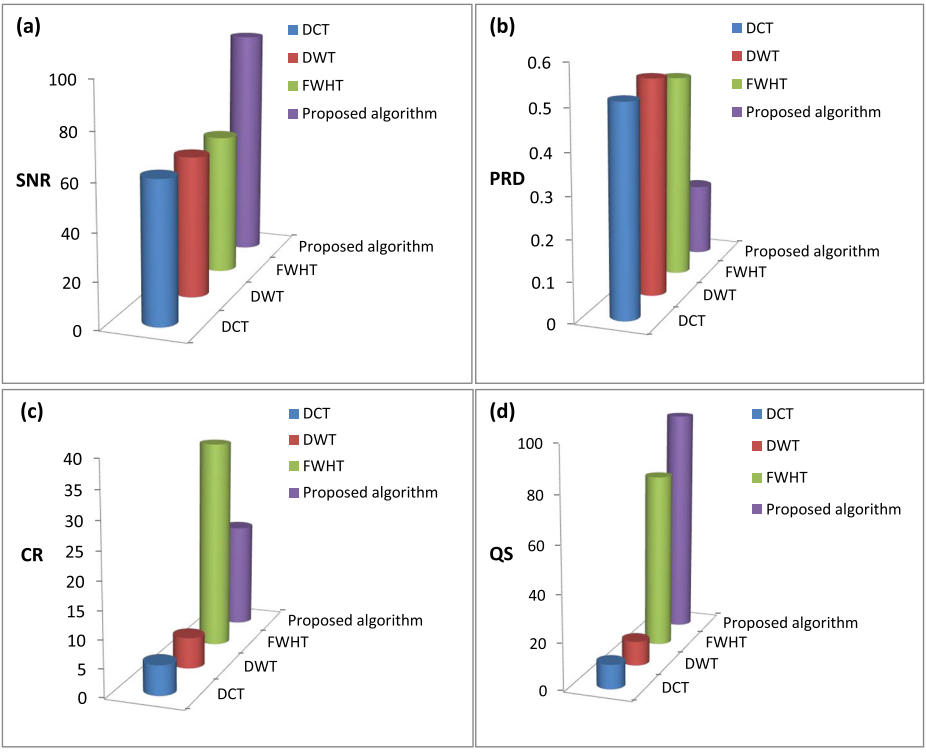

Fig. 7 Performance comparison of the proposed algorithm with DCT, DWT, and FWHT in the team of (**a**) SNR, (**b**) PRD, (**c**) CR (**d**) QS

7 Discussions

Experiments and the results above demonstrate that the proposed algorithm outperforms previous recent algorithms. Various metrics of performance were tested in the experiments. In the first place, we must consider the compression ratio and the quality of the compressed signals. Second, we considered the Compression time, Compression speed, and computational

Table 3 The Compression time, Compression speed, and computational efficiency of the proposed algorithm

FPCG signal	CR	Compression Time(s)	Compression Speed(bps)	CE
fetal_PCG_p01_GW_36m	16	1.47	177,600	10.88
fetal_PCG_p04_GW_38m	32	1.16	224,336	27.58
fetal_PCG_p05_GW_34m	32	1.32	197,328	24.24
fetal_PCG_p07_GW_38m	32	1.35	193,744	23.70
fetal_PCG_p11_GW_37m	32	1.16	244,336	27.58
fetal_PCG_p12_GW_39m	16	1.14	229,160	14.0.4
fetal_PCG_p15_GW_36m	16	1.12	234,192	14.28
fetal_PCG_p19_GW_38m	16	1.04	250,728	15.38
fetal_PCG_p23_GW_38m	32	1.08	244,176	29.63
fetal_PCG_p25_GW_37m	32	1.23	213,120	26.02
Average	**25.6**	**1.207**	**218,672**	**21.157**

efficiency. The last path is one of decreasing energy consumption. The tabular and graphical results demonstrate the efficacy of the suggested method in terms of all paths' performance measurements. The good results in compression ratio and compressed signals quality of the proposed algorithm it goes back to using discrete Charlier moment as a feature descriptor with the householder orthonormalization method (HOM). HOM preserves the orthogonal property of Charlier moment at high order; subsequently, the numerical error propagation doesn't occur when computing high-order Charlier moments. As a result, the proposed algorithm can achieve a high compression ratio and high quality of the compressed signals. The superiority in Compression time, Compression speed, and computational efficiency are thanks to using a recurrence relation completely independent of Charlier polynomials computation, which is no longer dependent on the factorial and power functions. In addition, using HOM in the proposed algorithm leads to speeding the compression, which is considered the best way of QR decomposition in signal reconstruction quality and execution time [27].

The average value of the performance metrics is CR = 18.33, PRD = 0.21, SNR = 48.85, PSNR = 68.86, and QS = 90.88. Even though the proposed algorithm didn't provide the highest CR, it did provide the best PRD, SNR, PSNR, and QS. This guarantees that the reconstructed signal has all relevant diagnostic information. This is important when compressing medical signals since losing diagnostic information could lead to a wrong diagnosis. Additionally, the superiority of the proposed approach in terms of compression time, compression speed, and computational efficiency makes it more efficient in decreasing energy consumption.

The superiority in the performance of the proposed approach in compressing fPCG signals can be attributed to the following factors:

- A Charlier moment has a basic function that is orthogonal to the moment. Each Charlier moment coefficient can capture the signal's distinct and unique components with no information redundancy.
- According to the order value, Charlier moments' basis functions can extract a variety of diverse forms of information from the signal. It is due to using the Householder orthonormalization method (HOM) to maintain the orthogonality property of Charlier polynomials.
- Moments generated from discrete orthogonal polynomials are effective at compressing signals. This is because they have a higher efficiency of energy compression for common signals. If the discrete orthogonal moment is correctly specified, the signal's energy is concentrated on a small fraction of the moment coefficients; these coefficients are then saved and used to reconstruct the signal.
- The power of Charlier moments to extract both local and global features.
- The higher compression speed and computational efficiency result from using recursive formulas to compute polynomials by lower polynomial orders instead of directly computing them.

There have been much advancement in compression techniques; however, there are still many obstacles to overcome. The computational complexity and the availability of memory management are two important factors in the development of compression techniques. Most current methods have high computing complexity, making them unsuitable for use in real-time applications like Remote Monitoring Systems. With the usage of the compression approach, memory management becomes more complicated. When the amount of memory

needed to do the compression method is more than what is available on the device, efficient compression cannot be done. Even if certain compression approaches obtain a higher CR, they do not manage memory effectively. So another interesting research topic is the study of memory management in compression algorithms.

8 Conclusion

The present article proposes a new compression technique for fPCG signals to reduce energy consumption in Remote Healthcare Monitoring systems (RHMS). The proposed compression algorithm employs Discrete Orthogonal Charlier Moment (DOCMs) as a features extractor due to the orthogonality of its basis functions. We determined and deleted the terms responsible for the numerical fluctuations in the values of the Charlier polynomial using a recurrence relation that is independent of the factorial and power functions for the construction of CPs. In order to preserve the orthogonality property of Charlier polynomials, the Householder orthonormalization method (HOM) is used. We evaluated the efficiency of proposed algorithm across Fetal PCG Database. It contains 26 fPCG signals from pregnant women in their final months of physiological singleton pregnancies (weeks 31–40). We used several metrics to compare the proposed algorithm to other well-known compression algorithms. The evaluation performance for the compression algorithm is implemented in three aspects. First, the compression ratio with reconstruction quality. Second, the compression speed and computational efficiency of the proposed algorithm. The third and final aspect is the energy consumption. The comparison between the proposed algorithm and the previous recent algorithms demonstrates that the proposed algorithm is better than those used in the previous works with respect to all aspects. In addition, the evaluation of energy consumption indicates that the proposed compression algorithm decreases the overall work time of devices in RHMS. In terms of the mentioned three aspects, our proposed algorithm satisfies the following: significant compression ratio is plausible, the quality of the reconstructed signal is respected, and energy consumption is decreased. As a result, it is well-suited for use with wearable devices, long-term data storage, massive databases, and RHMs.

In our future work, we may use new Discrete Orthogonal Moments as a feature extractor to improve the proposed algorithm for fPCG compression. Moreover, using various orthonormalization methods to maintain the orthogonality property at the High-order computation of Charlier polynomials could also increase the effectiveness of the proposed algorithm.

Funding Open access funding provided by The Science, Technology & Innovation Funding Authority (STDF) in cooperation with The Egyptian Knowledge Bank (EKB).

Data Availability The datasets generated and analysed during the current study are available in the following github repository: https://github.com/islam566/fPCG-signals-.

Declarations

Conflict of interest The authors declare that they have no Conflicts of interests.

References

1. Aazam M, Zeadally S, Harras KA (2020) Health fog for smart healthcare. IEEE Consum Electr Mag 9(2): 96–102. https://doi.org/10.1109/mce.2019.2953749
2. Abd Elaziz M, Hosny KM, Selim IM (2019) Galaxies image classification using artificial bee colony based on orthogonal Gegenbauer moments. Soft Comput 23(19):9573–9583. https://doi.org/10.1007/s00500-018-3521-2
3. Abdulhussain SH, Al-Haddad SAR, Mahmmod BM, Jassim WA (2017) On computational aspects of Tchebichef polynomials for higher polynomial order. IEEE Access 5:2470–2478. https://doi.org/10.1109/ACCESS.2017.2669218
4. Adithya PC, Sankar R, Moreno WA, Hart S (2017) Trends in fetal monitoring through phonocardiography: challenges and future directions. Biomed Signal Process Control 33:289–305. https://doi.org/10.1016/j.bspc.2016.11.007
5. Aggarwal V, Patterh MS, Singla VK (2018) Comparative studies of discrete cosine transform and lifting wavelet transform techniques for compression of blood pressure signal in salt sensitive dahl rat. Int J Comput Syst Eng 4(2-3):165–170. https://doi.org/10.1504/IJCSYSE.2018.091396
6. Aggarwal, V, Gupta, S, Patterh, MS, Kaur, L (2020) Analysis of compressed foetal phono-cardio-graphy (PCG) signals with discrete cosine transform and discrete wavelet transform. IETE J Res, 1–7https://doi.org/10.1080/03772063.2020.1725662.
7. Akram MU, Shaukat A, Hussain F, Khawaja SG, Butt WH (2018) Analysis of PCG signals using quality assessment and homomorphic filters for localization and classification of heart sounds. Comput Methods Prog Biomed 164:143–157. https://doi.org/10.1016/j.cmpb.2018.07.006
8. Altaheri H, Muhammad G, Alsulaiman M, Amin SU, Altuwaijri GA, Abdul W, ... Faisal M (2021) Deep learning techniques for classification of electroencephalogram (EEG) motor imagery (MI) signals: a review. Neural Comput Appl 1–42. https://doi.org/10.4018/JOEUC.2021010102
9. Arican M, Polat K (2019) Pairwise and variance based signal compression algorithm (PVBSC) in the P300 based speller systems using EEG signals. Comput Methods Prog Biomed 176:149–157. https://doi.org/10.1016/j.cmpb.2019.05.011
10. Atteeq, M, Khan, MF, Qureshi, AN (2019) Fetus heart beat extraction from Mother's PCG using blind source separation. In proceedings of the 2019 11th international conference on bioinformatics and biomedical technology (pp. 100-104). https://doi.org/10.1145/3340074.3340087
11. Bendifallah, A, Boulemden, M, Benzid, R (2015) Bitmask and SPIHT based PCG signal compression. In 2015 4th international conference on electrical engineering (ICEE) (pp. 1-4). IEEE. https://doi.org/10.1109/INFOCOM.2105.7218536.
12. Benouini R, Batioua I, Zenkouar K, Zahi A, El Fadili H, Qjidaa H (2019) Fast and accurate computation of Racah moment invariants for image classification. Pattern Recogn 91:100–110. https://doi.org/10.1016/i.patcog.2019.02.014
13. Bhatti UA, Huang M, Wu D, Zhang Y, Mehmood A, Han H (2019) Recommendation system using feature extraction and pattern recognition in clinical care systems. Enterp Inf Syst 13(3):329–351. https://doi.org/10.1080/17517575.2018.1557256
14. Cesarelli M, Ruffo M, Romano M, Bifulco P (2012) Simulation of foetal phonocardiographic recordings for testing of FHR extraction algorithms. Comput Methods Prog Biomed 107(3):513–523. https://doi.org/10.1016/j.cmpb.2011.11.008
15. Chien YR, Hsu KC, Tsao HW (2020) Phonocardiography signals compression with deep convolutional autoencoder for telecare applications. Appl Sci 10(17):5842. https://doi.org/10.3390/app10175842
16. Chourasia VS, Tiwari AK (2013) Design methodology of a new wavelet basis function for fetal phonocardiographic signals. Sci World J 2013:1–12. https://doi.org/10.1155/2013/505840

17. Daoui A, Yamni M, Ogri OE, Karmouni H, Sayyouri M, Qjidaa H (2020) New algorithm for large-sized 2D and 3D image reconstruction using higher-order Hahn moments. Circuits, Syst Signal Process 39(9):4552–4577. https://doi.org/10.1007/s00034-020-01384-z
18. Daoui A, Yamni M, Karmouni H, Sayyouri M, Qjidaa H (2020) Stable computation of higher order Charlier moments for signal and image reconstruction. Inf Sci 521:251–276. https://doi.org/10.1016/j.ins.2020.02.019
19. Daoui A, Karmouni H, Sayyouri M, Qjidaa H (2021) Fast and stable computation of higher-order Hahn polynomials and Hahn moment invariants for signal and image analysis. Multimed Tools Appl 80(21):32947–32973. https://doi.org/10.1007/s11042-21-11206-2
20. Daoui A, Sayyouri M, Qjidaa H (2021) Efficient computation of high-order Meixner moments for large-size signals and images analysis. Multimed Tools Appl 80(2):1641–1670. https://doi.org/10.1007/s11042-020-09739-z
21. Daoui A, Karmouni H, Sayyouri M, Qjidaa H (2022) Efficient methods for signal processing using Charlier moments and artificial bee Colony algorithm. Circuits, Syst Signal Process 41(1):166–195. https://doi.org/10.1007/s00034-021-01764-z
22. Daoui A et al (2022) On computational aspects of high-order dual Hahn moments. Pattern Recogn 127:108596. https://doi.org/10.1016/j.patcog.2022.108596
23. Elgendi M, Mohamed A, Ward R (2017) Efficient ECG compression and QRS detection for e-health applications. Sci Rep 7(1):1–16. https://doi.org/10.1038/s41598-017-00540
24. Ernawan F, Kabir N, Zamli KZ (2017) An efficient image compression technique using Tchebichef bit allocation. Optik 148:106–119. https://doi.org/10.1016/j.ijleo.2017.08.007
25. FATHI, Islam S., et al. (2022) An energy-efficient compression algorithm of ECG signals in remote healthcare monitoring systems. IEEE Access 10:39129–39144. https://doi.org/10.1109/ACCESS.2022.3166476
26. Fathi IS, Ahmed MA, Makhlouf MA, Osman EA (2021) Compression Techniques of Biomedical Signals in Remote Healthcare Monitoring Systems: A Comparative Study. Int J Hybrid Inf Technol 1(1):33–50. https://doi.org/10.21742/IJHIT.2021.1.1.03
27. Fathi IS, Ahmed M, Makhlouf M (2022) An efficient computation of discrete orthogonal moments for bio-signals reconstruction. EURASIP J Adv Signal Process 104(2022). https://doi.org/10.1186/s13634-022-00938-4
28. Ford W (2014) Numerical linear algebra with applications: using MATLAB. Academic Press is an imprint Elsevier 978-0-12-394435-1,1-628. https://doi.org/10.1016/B978-0-12-394435-1.0000-X
29. Ghosh SK, Ray A, Tripathy RK, Ponnalagu RN (2021) A transform domain approach for the compression of fetal phonocardiogram signal. IEEE Sensors Lett 5(5):1–4. https://doi.org/10.1109/LSENS.2021.3074985
30. Habibzadeh H, Dinesh K, Shishvan OR, Boggio-Dandry A, Sharma G, Soyata T (2019) A survey of healthcare internet of things (HIoT): a clinical perspective. IEEE Internet Things J 7(1):53–71. https://doi.org/10.1109/jiot.2019.2946359
31. Hassan G, Hosny KM, Farouk RM, Alzohairy AM (2020) An efficient retrieval system for biomedical images based on radial associated Laguerre moments. IEEE Access 8:175669–175687. https://doi.org/10.1109/ACCESS.2020.3026452
32. Hosny KM, Khalid AM, Mohamed ER (2018) Efficient compression of bio-signals by using Tchebichef moments and artificial bee Colony. Biocybernetics Biomed Eng 38(2):385–398. https://doi.org/10.1016/i.bbe.2018.02.006
33. Hosny KM, Khalid AM, Mohamed ER (2020) Efficient compression of volumetric medical images using Legendre moments and differential evolution. Soft Comput 24(1):409–427. https://doi.org/10.1007/s00500-019-03922-7
34. https://physionet.org/cgi-bin/atm/ATM
35. Jezewski M, Czabanski R, Horoba K, Leski J (2016) Clustering with pairs of prototypes to support automated assessment of the fetal state. Appl Artif Intell 30(6):572–589. https://doi.org/10.1080/08839514.2016.1193718
36. Jezewski M, Czabanski R, Leski JM, Jezewski J (2019) Fuzzy classifier based on clustering with pairs of ε-hyperballs and its application to support fetal state assessment. Expert Syst Appl 118:109–126. https://doi.org/10.1016/j.eswa.2018.09.030
37. Jha CK, Kolekar MH (2021) Empirical mode decomposition and wavelet transform based ECG data compression scheme. IRBM 42(1):65–72. https://doi.org/10.1016/j.irbm.2020.05.008
38. Karmouni H, Hmimid A, Jahid T, Sayyouri M, Qjidaa H, Rezzouk A (2018) Fast and stable computation of the Charlier moments and their inverses using digital filters and image block representation. Circuits, Syst Signal Process 37(9):4015–4033. https://doi.org/10.1016/j.ins.2020.02.019

39. Ladrova M, Sidikova M, Martinek R, Jaros R, Bilik P (2019) Elimination of interference in phonocardiogram signal based on wavelet transform and empirical mode decomposition. IFAC-PapersOnLine 52(27): 440–445. https://doi.org/10.3390/s20133790
40. Li T, Li J, Liu J, Huang M, Chen YW, Bhatti UA (2022) Robust watermarking algorithm for medical images based on log-polar transform. EURASIP J Wirel Commun Netw 2022(1):1–11. https://doi.org/10.1186/s13638-022-02106-6
41. Li Y, Li J, Shao C, Bhatti UA, Ma J (2022) Robust multi-watermarking algorithm for medical images using patchwork-DCT. In international conference on artificial intelligence and security (pp. 386–399). Springer, Cham. https://doi.org/10.1007/978-3-031-06791-4_31
42. Liu W, Li J, Shao C, Ma J, Huang M, Bhatti UA (2022) Robust zero watermarking algorithm for medical images using local binary pattern and discrete cosine transform. In international conference on artificial intelligence and security (pp. 350–362). Springer, Cham. https://doi.org/10.1007/978-3-031-06764-8_28
43. Martinek R, Kahankova R, Jezewski J, Jaros R, Mohylova J, Fajkus M, Nazeran H (2018) Comparative effectiveness of ICA and PCA in extraction of fetal ECG from abdominal signals: toward non-invasive fetal monitoring. Front Physiol 9:648. https://doi.org/10.3389/fphys.2018.00648
44. Martinek R, Barnova K, Jaros R, Kahankova R, Kupka T, Jezewski M, Horoba K (2020) Passive fetal monitoring by advanced signal processing methods in fetal phonocardiography. IEEE Access 8:221942–221962. https://doi.org/10.22489/CinC.2017.331-075
45. Mozaffarian D, Benjamin EJ, Go AS, Arnett DK, Blaha MJ, Cushman M, Turner MB (2016) Heart disease and stroke statistics—2016 update: a report from the American Heart Association. Circ 133(4):e38–e360. https://doi.org/10.1161/CIR.0000000000000350
46. Rahman SM, Howlader T, Hatzinakos D (2016) On the selection of 2D Krawtchouk moments for face recognition. Pattern Recogn 54:83–93. https://doi.org/10.1016/j.patcog.2016.01.003
47. Rajasekar P, Pushpalatha M (2020) Huffman quantization approach for optimized EEG signal compression with transformation technique. Soft Comput 24(19):14545–14559. https://doi.org/10.1007/s00500-020-04804-z
48. Sbrollini, A, Strazza, A, Caragiuli, M, Mozzoni, C, Tomassini, S, Agostinelli, A, Burattini, L (2017) Fetal phonocardiogram denoising by wavelet transformation: robustness to noise. In 2017 computing in cardiology (CinC) (pp. 1-4). IEEE. https://doi.org/10.22489/CinC.2017.331-075.
49. Stojkoska, BR, Nikolovski, Z (2017) Data compression for energy efficient IoT solutions. In 2017 25th telecommunication forum (TELFOR) (pp. 1-4). IEEE. https://doi.org/10.1109/TELFOR.2017.8249368.
50. Strand S, Lutter W, Strasburger JF, Shah V, Baffa O, Wakai RT (2019) Low-cost fetal magnetocardiography: a comparison of superconducting quantum interference device and optically pumped magnetometers. J Am Heart Assoc 8(16):e013436. https://doi.org/10.1161/JAHA.119.013436
51. Tang H, Zhang J, Sun J, Qiu T, Park Y (2016) Phonocardiogram signal compression using sound repetition and vector quantization. Comput Biol Med 71:24–34. https://doi.org/10.1016/j.compbiomed.2016.01.017
52. Tsung-Han T, Fong-Lin T (2022) Efficient lossless compression scheme for multi-channel ECG signal processing. Biomed Signal Process Control 59(2020):101879. https://doi.org/10.1016/j.bspc.2020.101879
53. Vadali, VABK (2018) A comparative study of signal processing methods for fetal phonocardiography analysis. University of South Florida. https://digitalcommons.usf.edu/etd/7373.
54. Welba C, Okassa AJO, Eloundou PN, Ele P (2020) Contribution to S-EMG signal compression in 1D by the combination of the modified discrete wavelet packet transform (MDWPT) and the discrete cosine transform (DCT). J Signal Inf Process 11(3):35–57. https://doi.org/10.4236/jsip.2020.113003
55. Xiao B, Lu G, Zhang Y, Li W, Wang G (2016) Lossless image compression based on integer discrete Tchebichef transform. Neurocomputing 214:587–593. https://doi.org/10.1016/j.neucom.2016.06.050
56. Xiao B, Luo J, Bi X, Li W, Chen B (2020) Fractional discrete Tchebyshev moments and their applications in image encryption and watermarking. Inf Sci 516:545–559. https://doi.org/10.1016/j.ins.2019.12.044
57. Yamni M, Daoui A, Karmouni H, Sayyouri M, Qjidaa H, Flusser J (2020) Fractional Charlier moments for image reconstruction and image watermarking. Signal Process 171:107509. https://doi.org/10.1016/j.sigpro.2020.107509
58. Zeng, C, Liu, J, Li, J, Cheng, J, Zhou, J, Nawaz, SA, ... & Bhatti, UA (2022) Multi-watermarking algorithm for medical image based on KAZE-DCT. J Ambient Intell Human Comput, 1–9. https://doi.org/10.1007/s12652-021-03539-5.
59. Zhu H, Liu M, Shu H, Zhang H, Luo L (2010) General form for obtaining discrete orthogonal moments. IET Image Process 4(5):335–352. https://doi.org/10.1155/2018/1673283